

EVOLUTION OF THE MICROSTRUCTURAL PARAMETERS OF COLD WORK Ti-6-Al-4V ALLOY

Brahim Mehdi^{1,2)*}, Nabil Kherrouba¹⁾, Soumia Doufana^{1,2)}, Riad Badji¹⁾, Baya Alili³⁾

¹Research Center in Industrial Technologies CRTI, P. O. Box 64, Cheraga, Algeria

²Ecole Nationale Supérieure des Mines et de la Métallurgie-Annaba Sidi Amar Chaiba (Ex : CEFOS), BP 233 RP Annaba 23000, Algeria

³Faculté de Physique, USTHB, BP 32 El-Alia, Dar El Beida, Alger, Algérie.

*Corresponding author: e-mail: m_mehdi76@yahoo.fr. Tel.: +213 54 072 4466, Research Center in Industrial Technologies CRTI, P. O. Box 64, Cheraga, Algeria.

Received: 12.05.2017

Accepted: 08.10.2017

*Corresponding author: e-mail: b.mehdi@crti.dz, m_mehdi76@yahoo.fr. Tel.: +213 54 072 4466, Research Center in Industrial Technologies CRTI, P. O. Box 64, Cheraga, Algeria.

Abstract

The aim of this work is to investigate cold worked Ti-6Al-4V ($\alpha+\beta$) alloy. The alloy was examined by X-ray diffraction using Rietveld refinement method. MAUD software (Materials Analysis Using Diffraction) was used to analyze the microstructural parameters evolution (crystallite size, root mean square strain (r.m.s) and dislocation density. The Crystallite size is smaller in the β -phase compared to the α -phase. Microstrain and dislocation density are higher in the α -phase than those found in the β -phase for the as received material. The microstructural parameters of Ti-6Al-4V alloy exhibit typical values of cold deformation state. The results show that the deformation process reduces the crystallite size (coherent diffraction domains) from 520 to 210 Å in the α -phase. Consequently, the r.m.s increases from 5 E^{-4} to 32 E^{-4} and the dislocation density increases from 2.92 E^{+10} to $4.6 \text{ E}^{+11} \text{ m}^{-2}$ after 85 % thickness reduction.

Keys words: Ti-6Al-4V alloy, cold working, crystallite size, dislocation density

1 Introduction

Ti-6Al-4V is one of the most used $\alpha+\beta$ titanium alloys, which is employed in many industries (aeronautic, aerospace, blades, discs, rings, airframes, fasteners, components, vessels, cases, hubs, forgings, biomedical implants), due to its attractive mechanical properties [1-5]. The intensive utilization of this alloy requires the control of microstructural parameters during cold working. Nowadays, titanium alloys have matured rapidly and it is more interesting than other structural materials. Cold rolling is generally used as the plastic deformation processing of these alloys. Crystallite size, r.m.s strain and dislocation density are very important factors controlling the microstructure evolution during plastic deformation. Different X-ray Diffraction Line Profile Analysis (XRDLPA) techniques have been widely applied successfully for the evaluation of microstructural parameters in deformed metals and alloy systems [6-14]. Recently, it was established that XRDLPA is a very useful technique to characterize deformed microstructures [15, 16]. In this work, the microstructural parameters evolution after cold rolling of Ti-6Al-4V was studied. Two cold plastic deformation levels, 50% and 85% (thickness reduction) were investigated. To achieve this work, XRDLPA was carried out using JAVA-based Materials Analysis Using Diffraction (MAUD) software [17-18].

2 Material and experimental Procedures

A commercial Ti-6Al-4V sheet is used. The nominal chemical composition of this alloy is presented in **Table 1**. The Ti-6Al-4V sheets are hot rolled until 2 mm of thickness. The alloy underwent plastic deformation by cold rolling with 50 and 85% thickness reduction. The X-ray diffraction XRD patterns have been recorded from the rolled and polished samples' surface using BRUKERS D2 Phaser second generation benchtop X-Ray Diffractometer operating at 30 kV, 30 mA with Co K_{α} radiation. All the diffraction patterns were obtained by varying 2θ from 20° to 120° with a scan step of 0.02. The time spent for collecting the data per step was 5 s. After this, MAUD software, which is based on a Rietveld refinement procedure, was used.

Table 1 Chemical composition of the as received alloy

Elements	weight (%)
Al	6.75
V	4.5
C	0.05
H	0.015
O	0.18
N	600
Fe	0.30

3 Results

Fig. 1 presents the XRD patterns obtained from the as received Ti-6Al-4V alloy with the presence of the characteristic diffraction peaks associated to the α -HCP and β -BCC phases.

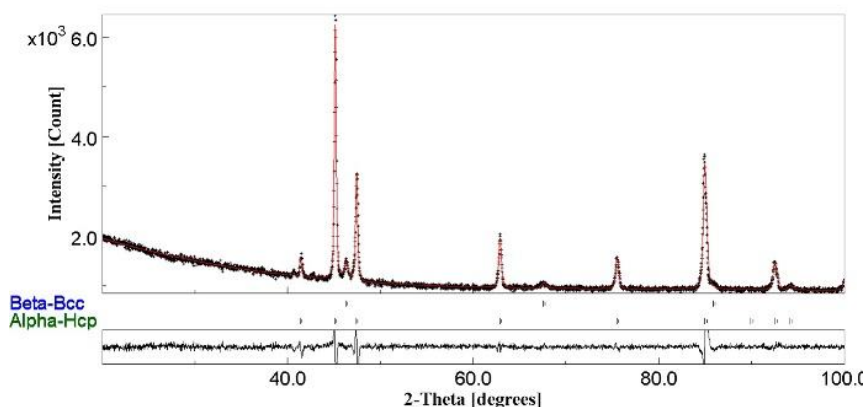


Fig. 1 XRD obtained from Rietveld profile fitting of the as received Ti-6Al-4V alloy

Fig. 2 and **Fig. 3** show the XRD patterns of the cold rolled samples, the presence of the peaks associated to α -phase and the absence of all the peaks associated to the β -phase after cold rolling are clearly noticed. This can be explained by the low volume fraction of the β phase and the reduction in the size of coherent domains of diffraction. In addition, the crystalline anisotropy of the studied alloy contributes in the absence of peaks associated to the β -phase.

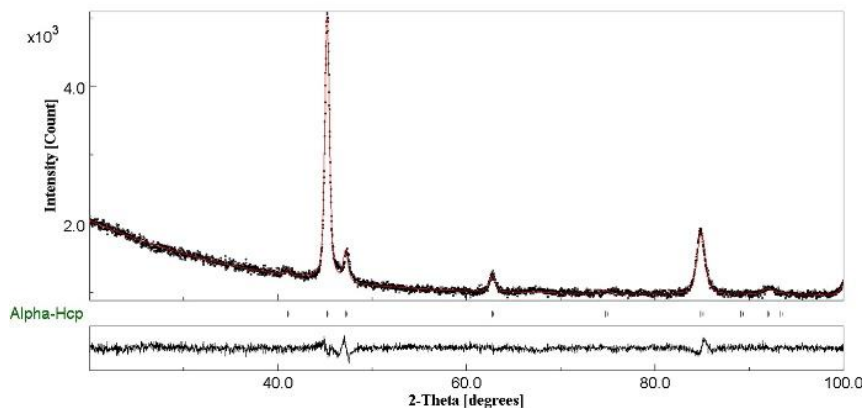


Fig. 2 XRD patterns obtained from Rietveld profile fitting of Ti-6Al-4V alloy cold rolled up to 50 %

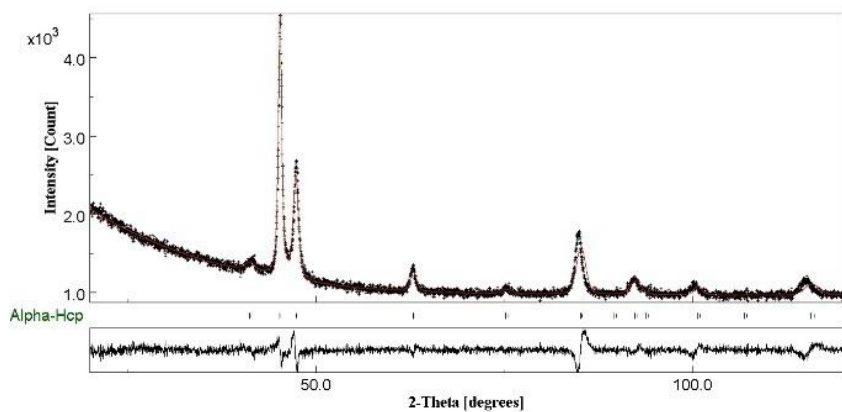


Fig. 3 XRD patterns obtained from Rietveld profile fitting of Ti-6Al-4V alloy cold rolled up to 85 %.

Table 2 Values of microstructural parameters obtained from Rietveld analysis

Samples	Phases	Lattice parameters (Å)	Crystallite size D (Å)	r.m.s E ⁻⁴	Dislocation density E ⁺¹⁰	Goodness of fit	Fit Parameters
As received	α-Hcp	a = 2.927 c = 4.673	520	0.05	2.92	0.99	Rb: 2.18 Rexp:2.91 Rwp: 2.90
	β-Cc	a= 3.224	125	0.02	0.05	0.99	Rb: 2.01 Rwp: 2.90
Rolled 50 %	α-Hcp	a = 2.945 c = 4.671	380	26	21	0.90	Rexp:2.85 Rb:1.94 Rwp:2.57
Rolled 85 %	α-Hcp	a = 2.945 c = 4.679	210	32	46	0.85	Rexp: 2.88

The XRD patterns of all the specimens were subjected to detailed microstructural analysis using MAUD software as shown in **Table 2**. It is obvious that, β -phase at the as received state exhibit smaller domain size than the α -phase. These observations are reminiscent to the low volume fraction of the β -phase. Moreover, the domain size for the α -phase are smaller than that of the corresponding α -phase in the case of the two deformed states (50 and 85 % thickness reduction) and decrease from 520 to 210 Å after 85 % of thickness reduction. This is accompanied by an increase in the microstrain and dislocations density values with increasing the deformation amount.

4 Discussion

The GOF (Goodness Of Fit) value, which is an indicator of the fit quality strongly depends on all the values of the parameters obtained by the Rietveld analysis. This value oscillates, for the studied alloy between 0.99 and 0.85 with a mean value of 0.95, which is very close to 1.3 indicating the high quality of the fit according to the literature. The values of Rwp (%) and Rexp (%), which are indicators of the precision of the refinement, are very good (less than 10%). The lattice parameters of the deformed alloy appear to be stable. This stability of the lattice parameters is explained by the absence of any physical change (for instance an increase in the concentration of one of the solute atoms (Al or V)) that could modify the lattice parameters. Indeed, thermomechanical treatments (rolling and aging) have no effect on the lattice parameters, whose variation is only sensitive to the effects of electronic linkages of the chemical species. It is noted that thermal agitation also affects the lattice parameters. After deformation, the disappearance of the peaks associated to the B-cc structure is observed. This can be explained by the small volume fraction of the β phase with strong deformation at the local scale. Consequently, small values of coherent domain size were obtained after deformation and cold working. Subsequently, only the evolution of the microstructural parameters of α phase was examined (an overall decrease in the sizes of the domains as a function of the deformation rate is noticed). It is known that the higher the deformation, the lower the coherent diffraction domains size, consequently the micro distortions in the material increases as a function of the rolling rate. The immediate fact to note is the increase in the density of dislocations as a function of the rolling rate, which is explained by a mechanism of hardening by gathering the dislocations in walls and forests. **Fig. 4** shows effect of the deformation on the crystallite sizes and the dislocations density; the higher the deformation, the lower the crystallite size and the higher the dislocations density. The same tendency was also observed in the literature [19-20].

It was reported [21] that, some experimental observations from the X-ray analysis regarding the dislocation substructure evolution is explained by considering the basic deformation mechanism of the two-phase materials. During deformation, most of the dislocation assisted slip activities will occur in the α -phase. Thus, when the deformation rate increases, the activity of slip systems increases, and, consequently, dislocation density increases. An important finding of X-ray analysis is that in the deformed Ti-6Al-4V alloy, there is an increase of the dislocations density in the α phase. The plastic deformation could introduce much higher dislocations into the material and the substitution elements in the alloy seems to lead to drastic changes on post deformation [22]. In this work, the dislocations density increases from 2.92 E^{+10} to 4.6 E^{+11} when the plastic deformation was more important.

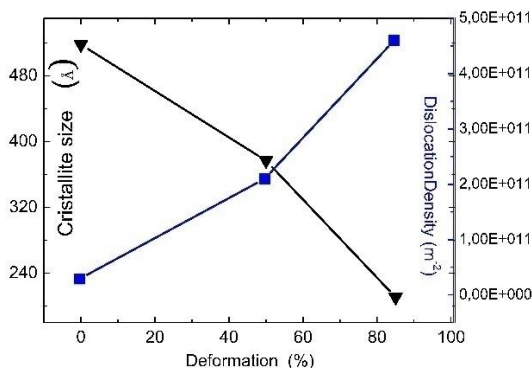


Fig. 4 Evolution of the crystallite size and dislocation density in the deformed samples

5 Conclusion

In this work, the microstructural parameters evolution of the cold worked Ti-6Al-4V alloy was examined by X-ray diffraction using Reitveld method. Parameters like crystallite size, microstrain and dislocations density within the domains have been characterized.

- The results indicate that the crystallite size is smaller in the case of the β -phase compared to the corresponding α -phase and the microstrain and dislocations density are higher in the α phase than in the β -phase in the as received material.
- The crystallite size decreases while the microstrain and dislocation density increases with the deformation amount. The dislocations density increases from 2.92 E^{+10} to 4.6 E^{+11} (factor of 10) when the deformation amount reaches 85 %.

References

- [1] D. Banerjee, J.C. Williams: *Acta Materialia*, Vol. 61, 2013, p. 844–879, DOI: 10.1016/J.ACTAMAT.2012.10.043.
- [2] H.W. Song, S.H. Zhang, M. Cheng: *Transactions of Nonferrous Metals Society of China*, Vol 20, Issue 11, 2010, p. 2168-2173, DOI: 10.1016/S1003-6326(09)60437-4
- [3] B. Poorganji et al.: *Scripta Materialia*, Vol 61, 2009, No. 4, p. 419-422, DOI: 10.1016/J.SCRIPTAMAT.2009.04.033.
- [4] I. Weiss, F.H. Froes, D. Eylon, G.E. Welsch: *Metallurgical Transactions A*, Vol. 17, 1986, No. 11, p. 1935–1947, DOI: 10.1007/BF02644991
- [5] M. A. Vicente Alvarez, J. R. Santisteban, P. Vizcaíno, G. Ribarik, T. Ungar: *Acta Materialia*, Vol. 117, 2016 p. 1-12, DOI: 10.1016/J.ACTAMAT.2016.06.058
- [6] N. Naga Krishna, R. Tejas, K. Sivaprasad, K. Venkateswarlu: *Materials and Design*, Vol. 52, 2013, p. 785–790, DOI: 10.1016/j.matdes.2013.05.095
- [7] K. Maniammal, G. Madhu, V. Biju: *Physica E*, Vol. 85, 2017, p. 214–222, DOI:10.1016/J.PHYSE.2016.08.035
- [8] M. Abdellatif, M. Abele, M. Leoni, P. Scardi: *Thin Solid Films*, Vol. 530, 2013, p. 44–48, DOI: 10.1016/J.TSF.2012.09.020
- [9] P. Mukherjee, A. Sarkar, P. Barat: *Materials Characterization*, Vol. 55, 2005, p. 412–417, DOI: 10.1016/J.MATCHAR.2005.09.002

- [10] P. Mukherjee, A. Sarkar, M. Bhattacharya, N. Gayathri, P. Barat: *Journal of Nuclear Materials*, Vol. 395, 2009, p. 37–44, DOI: 10.1016/J.JNUCMAT.2009.09.013
- [11] P. Mukherjee, N. Gayathri, P. S. Chowdhury, M. K. Mitra: *Journal of Nuclear Materials*, Vol. 434, 2013, p. 24–30, DOI: 10.1016/j.jnucmat.2012.11.028
- [12] F. Abouhilou, A. Khereddine, B. Alili, D. Bradai: *Transactions. Nonferrous Metals. Society of China*, Vol. 22, 2012, p. 604–607, DOI: 10.1016/S1003-6326(11)61220-X
- [13] A. R. Bushroa, R. G. Rahbari, H. H. Masjuki, M.R. Muhamad: *Vacuum*, Vol. 86, No. 8, 2012, p. 1107–1112, DOI: 0.1016/J.VACUUM.2011.10.011
- [14] A. Y Khereddine, F. HadjLarbi, M. Kawasaki, T. Baudin, D. Bradaia, T. G. Langdon, *Materials Science and Engineering A*, Vol. 576, 2013, p. 149–155, DOI: 10.1016/j.msea.2013.04.004
- [15] J. Gubicza, L. Balogh, R.J. Hellmig, Y. Estrin, T. Ungar: *Materials Science and Engineering A*, Vol. 400–401, 2005, p. 334–338, DOI:10.1016/j.msea.2005.03.042
- [16] L. Lutterotti: MAUD. Cpd Newsletter, (IUCr), 2000, Vol. 24
- [17] <http://www.ing.unitn.it/~luttero/>.MAUD: Material Analysis Using Diffraction
- [18] A. Dutta Gupta et al.: *Nuclear Instruments and Methods in Physics Research Section B: Beam Interactions with Materials and Atoms*, Vol. 387, 2016, p. 63–72, DOI: 10.1016/J.NIMB.2016.09.010
- [19] A. Sarkar, P. Mukherjee, P. Barat: *Materials Sciences Engineering A*, Vol. 485, 2008, p. 176–81, DOI: 10.1016/J.MSEA.2007.07.063
- [20] A. Sarkar, R. Shibayan, S. Satyam: *Materials Characterization*, No. 62, 2011, p. 35–42, DOI: 0.1016/j.MATCHAR.2010.10.007
- [21] A. Khereddine, F. Hadj-Larbi, L. Djebala, H. Azzeddine, B. Alili, D. Bradai: *Transactions. Nonferrous Metals. Society of China*, Vol. 21, No. 3, 2011, p. 482–487, DOI: 10.1016/S1003-6326(11)60740-1